http://dx.doi.org/10.15576/GLL/2023.4.97

GLL

Geomatics, Landmanagement and Landscape No. 4 • 2023, 97–112

A MATHEMATICAL APPROACH TO CALCULATING SLOPE STABILITY UNDER PHYSICAL TRIGGERING FORCES. APPLICATION TO LANDSCAPE MECHANICS

Larbi Khaber, Karim Zighmi, Riheb Hadji

Summary

In the field of land management, the limit equilibrium calculation method is a mathematical method that harmonizes the complex interplay of diverse factors determining the slope stability. Rooted in mechanical and mathematical principles, this method has paramount significance for guiding the course of safe land management in mountainous regions, especially in the case of infrastructure development projects. Conventional limit equilibrium techniques, while providing preliminary stability assessments, often neglect key factors that can trigger slope failure. These approaches traditionally ignore the spatial variations in soil properties, the temporal dynamics of phenomena, the kinetic responses to external loads, the complexities of geological formations, and the influences of the hydrological and climatic conditions on slope stability. Our innovative method adopts an enriched mathematical framework that redefines the landscape of force equilibrium techniques. We meticulously tailor this framework by adapting the foundational relationships derived from the Mohr-Coulomb shear strength criterion to accommodate the spatially variable geomechanical parameters. This adaptation allows us to capture the nuanced shifts in mechanical properties over the extent of the slope. Furthermore, we introduce supplementary equations that seamlessly integrate the influences of traffic-induced loads and hydraulic pressures, while also statistically quantifying the contributions of stabilizing structures. To determine the efficacy of this geomatic and landscape-centric numerical tool, we have subjected it to rigorous testing on a test slope. The outcomes derived from our mathematical model reveal the primacy of traffic-related forces as the main destabilizing agents, contrasted with the strengthening effects of reinforcements in maintaining slope stability.

Keywords

limit equilibrium ealculation • slope stability analysis • mathematical framework • geomechanical properties • infrastructure development

1. Introduction

Slope equilibrium is a central concern in geotechnical engineering, given the profound risks associated with mass wasting events. As hilly terrain is often the preferred choice for critical infrastructure development, a careful assessment of slope stability is essen-

tial for fostering resilient land use planning and effective hazard mitigation [Zahri et al. 2016, Fredj et al. 2020, Boubazine et al. 2022].

The utilization of applied mathematical tools to understand the physical and mechanical intricacies of slope stability is of paramount significance. It enables engineers to delve deeper into the underlying principles that govern slope behavior, thereby improving our ability to assess and manage these complex systems. In this context, limit equilibrium methods have retained their prominence as the preferred choice for slope stability analysis. These methods offer several advantages, in particular their ability to accommodate complicated geometries and varying soil saturation conditions [Kallel et al. 2018, Dahoua et al. 2018, Kerbati et al. 2020, Ncibi et al. 2021, Brahmi et al. 2021, Mahleb et al. 2022].

Among the established approaches to slope stability analysis, the methods of Bishop, Janbu, and Fellinuis have historically played a key role. However, it is imperative to recognize that while these conventional techniques provide reasonable estimations of failure surfaces, they have certain limitations. Notably, they tend to assume simplified intrinsic soil strength and often neglect critical triggering processes, thus potentially leading to conservative assessments of slope stability [Zekiri et al. 2019, Saadoune et al. 2022].

The adoption of the simplified Fellinuis and Bishop procedures in this study is justified. Both methods, with their foundations in limit equilibrium theory, provide valuable insights into slope stability. The Fellinuis and Bishop methods have gained favor due to their ability to satisfy the total moment equilibrium, as illustrated in Figure 1, which is crucial for capturing the essence of slope behavior under the influence of various forces.

How a slope behaves is governed by a complex interplay of hydro-geomorphological, geological, and anthropic factors under both natural and engineered conditions. Instabilities are often initiated by environmental perturbations such as seismic activity, precipitation, freeze-thaw cycles, and vegetation removal. Additionally, the development of infrastructure introduces further stresses due to traffic loads and construction activities [Hadji et al. 2013, Dahoua et al. 2017, Karim et al. 2019].

A number of key triggering processes, frequently neglected by conventional limit equilibrium methods, such as Fellinuis and Bishop, have a significant influence on slope stability. These processes include the geometric variability of soil shear strength properties (cohesion and friction angle) within the slope mass, variations in pore water/hydrostatic pressure, the impact of dynamic/cyclic loads (e.g., earthquakes, blasting, heavy traffic), progressive degradation of soil properties over time due to erosion and anthropic activities (e.g., road construction, slope cutting, refuse dumping), as well as the influence of climate and weathering (e.g., rainfall infiltration, freeze-thaw cycles, droughts) [Hadji et al. 2016, 2017, Manchar et al. 2018, Anis et al. 2019].

To address these complexities of slope stability, alternative approaches have been developed, each tailored to specific scenarios. These approaches range from finite element/discrete element methods, capable of modeling spatially variable soil properties and complex failure surfaces, to pseudo-static limit equilibrium methods that

incorporate seismic acceleration coefficients for earthquake loading considerations. Furthermore, finite difference/volume methods can dynamically simulate rainfall infiltration and coupled hydro-mechanical effects, while ring shear apparatus allows laboratory testing under cyclic/dynamic loading conditions. Probabilistic/stochastic analyses employ random field generators and Monte Carlo simulations to capture soil property variability, and back-analysis of historical failures integrates measured environmental factors, such as rainfall and groundwater levels. Numerical weathering models simulate polythermal, frost action, and desiccation stresses, while limit analysis and strain-softening models account for progressive strength loss. Hybrid techniques combine numerical modeling with limit equilibrium for fidelity assessments.

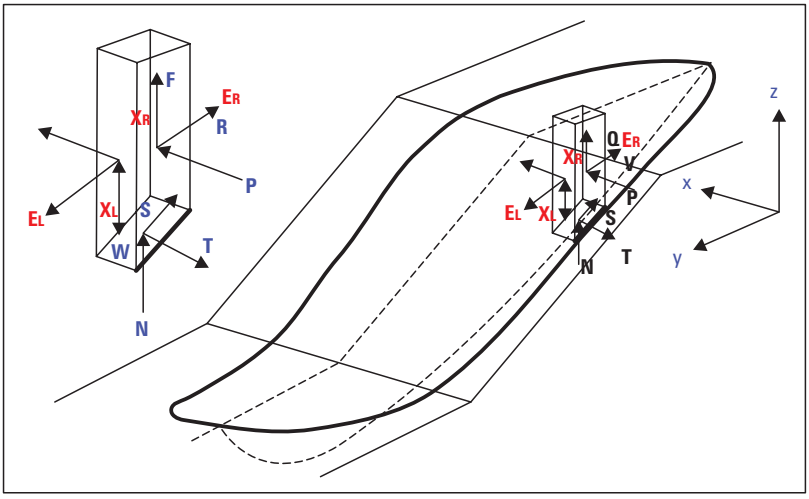

Source: Authors' own study

Fig. 1. Mechanism and components of a slope movement

This study attempts to pioneer an improved mathematical stability model framework, incorporating the previously neglected slope triggering mechanisms within a rigorously mechanistic formulation. By merging intrinsic and external forces, this framework enables the development of resilient land management strategies. The subsequent sections of this paper will describe the modifications to conventional limit equilibrium theory, with a focus on spatially variable soils, pore-water pressures, and anthropic loads.

The application of this framework to a test slope serves to demonstrate its ability to provide an improved characterization of the failure-driving processes, underscoring the importance of incorporating advanced mathematical tools for a holistic approach to slope stability analysis in the context of sustainable land management.

2. Fellinuis and Bishop mathematical approaches

The Fellinius method is one of the earliest equilibrium calculation methods developed.

It satisfies both the horizontal and vertical force equilibrium equations for each slice by assuming a functional relationship between the interslice shear force (τ) and the average normal stress (σ') across the base of that slice [Charles and Soares 1984].

The mathematical equation of the Fellinius method assumes that the ratio of the interslice shear force (τ) to the average normal stress (σ') is a constant k:

$$\tau/\sigma' = k \tag{1}$$

where:

τ – interslice shear force,
σ' – average normal stress across slice base
k – dimensionless constant.

To satisfy both the horizontal and vertical force equilibria, the value of k must be:

$$k = \tan(\varphi') \tag{2}$$

where: φ' – the effective angle of internal friction of the soil.

This assumption essentially models the shear strength behavior using a Mohr-Coulomb failure criterion. The factor of safety (F_S) against sliding is then calculated by force equilibrium.

Key advantages of the Fellinius method include its simplicity and its ability to consider complex geometries. However, it does not fully satisfy the moment equilibrium conditions.

The Bishop method assumes a linear distribution of shear stress along the base of each potential sliding mass slice. It satisfies both the force and the moment equilibrium for each slice [Bishop 1955].

The mathematical formulation of this method divides the sliding mass into a number of slices with bases perpendicular to the assumed failure surface. It assumes a trial factor of safety, Fs, and calculates the shear strength available to resist sliding for each slice:

$$\tau = c' + (\sigma' \tan\varphi')/Fs \tag{3}$$

where:

c' – effective cohesion,
σ' – average normal stress on slice base,
φ' – effective friction angle.

Calculate disturbing and driving forces (shear and normal stresses) on each slice.

Apply force equilibrium for each slice:

$$\Sigma\, \tau \text{ allow} = \Sigma\, \tau \text{ disturbing.}$$

Apply moment equilibrium around the center of rotation of each slice:

$$\Sigma M \text{ allow} = \Sigma M \text{ disturbing.}$$

The Bishop parameter, α, is introduced to satisfy both the force and the moment equilibrium simultaneously:

$$\tau = c' + (\sigma' \tan\varphi')(1 - \alpha) + \alpha(\sigma'b \tan\varphi') \quad (4)$$

where: σ'b – the normal stress on the slice base.

Iterate α and Fs until the force and the moment equilibrium are satisfied for all slices.

The Fs that satisfies both the force and the moment equilibrium is taken as the factor of safety.

Bishop fully satisfies both the force and the moment conditions using a parameter α to distribute shear stress linearly in each slice.

3. Mathematical/Physical methodology

3.1. Slope stability analysis

The assessment of slope stability is conducted through a meticulous limit equilibrium analysis. In this method, the potential failure mass is discretized into discrete slices, each based on the critical circular failure surface, as outlined by Terzaghi [1967]. For each slice, we apply force and moment equilibrium equations to quantify both stabilizing and driving stresses, as explained by Morgenstern and Price [1965].

3.2. Incorporating spatial variability

We account for the spatial variability of intrinsic soil properties by using probabilistic distributions of cohesion (c') and friction angle (φ'). These distributions are derived from extensive soil sampling. Instead of assigning uniform mean values to slice properties, we give random values from probability density functions to better represent real world variability.

3.3. Pore-water pressure modeling

Pore-water pressure is determined using a coupled hydrological-geomechanical modeling approach. The hydrological model simulates processes such as rainfall infiltration and snowmelt to generate transient pressure heads. The resulting positive and negative pore pressures acting on the slice bases are subsequently incorporated into the limit equilibrium analysis.

3.4. Dynamic analysis of traffic loading

The stresses induced by traffic loading are quantified by dynamic analysis of acceleration time-histories recorded at the site. Using wave propagation theory, equivalent dynamic

coefficients are estimated to represent the maximum speed-dependent accelerations. Horizontal and vertical forces are then introduced proportionally to slice mass, following the methodology proposed by Mestat [1998].

3.5. Modeling reinforcement forces

To account for reinforcement forces from inclusions, we employ mechanical modeling using beam elements connected between slice centroids. Normal and tangential reaction stresses along the inclusion-soil interfaces are incorporated into the probabilistic limit equilibrium formulation.

3.6. Satisfying static admissibility criteria

By iteratively applying techniques to satisfy static admissibility criteria, we rigorously determine the safety factor (Fs) against instability. This approach takes into account the spatially distributed intrinsic strengths and coupled triggering influences, allowing for a comprehensive assessment of slope stability.

3.7. Validation testing

The improved characterization of processes that create instability is confirmed through validation testing. This process ensures that our model is an accurate representation of slope behavior in the real world.

3.8. Modeling reinforcement inclusions in detail

Rigid inclusions: Inclusions such as piles and walls are discretized as linear beam elements connected between adjacent slope slice centroids.

3.9. Stress approximation

Normal and shear stresses acting along the inclusion-soil interface are approximated using linear elastic beam-soil contact theory.

Beam cross-sectional properties: Properties such as area and moment of inertia for the beam elements are defined based on the inclusion geometry.

3.10. Stiffness definition and external loads

The stiffness of the beam-soil interface is defined using the elastic moduli of the inclusion and the soil in contact. External loads acting on the inclusion, such as earth pressures, are applied at nodes.

3.11. Reactive stresses

Resultant reactive stresses from the beam are integrated along the inclusion-slice interface length.

3.12. Contribution to slice state

Normal stresses contribute to the effective stress state of the slice, while shear stresses are factored into resisted/driving shear stresses in limit equilibrium.

Iterative solution: An iterative solution process balances the forces within the slices while including the interlocking behavior of reinforced slice-inclusion systems.

3.13. Sensitivity analyses

Sensitivity analyses on inclusion properties and spacing allow us to assess the degree of stabilization provided. This approach captures the complex stress redistribution role of inclusions in a computationally efficient manner.

3.14. Real-world application

To demonstrate the practicality of our approach, we applied it to an actual project involving the design of a new highway along a steep clayey slope prone to rainfall-induced landslides. Our methodology involved collecting soil samples for shear strength testing, installing piezometers for pore pressure monitoring, and determining the critical failure surface using topographic data and geological mapping. We then divided the potential failure mass into slices along this surface, inputting shear strength distributions and groundwater pressures into the model.

3.15. Reinforcement design

The barrette reinforcements were modeled as longitudinal beam elements between slice centroids. We applied traffic load estimates based on site conditions and iterated inclusion geometry and stiffness parameters to achieve force/moment equilibrium with a design safety factor (Fs) exceeding 1.5.

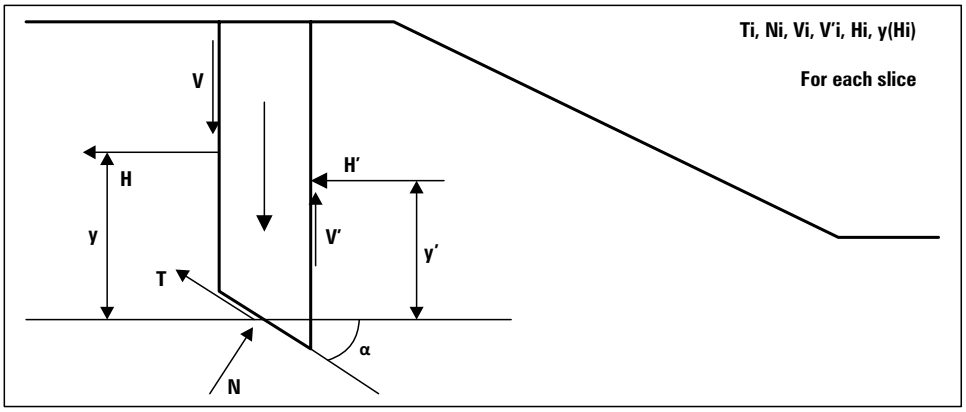

Source: Authors' own study

Fig. 2. The sliding body and the forces acting on it

4. Mathematical approach

In this study we propose a mathematical modification of the conventional Bishop's method, which aims to rigorously satisfy the principle of static admissibility through an extended formulation. In this improved approach, we maintain consistency of notation, provide clear explanations of variables and their physical meanings, and ensure proper consideration of units and dimensions.

4.1. Assumptions and simplifications

Our method begins with the assumption that circular failure surfaces govern the behavior of the sliding mass. To analyze slope stability, we discretize the sliding mass into vertical slices, each having a width represented by 'bi'.

4.2. Variables and constants

For each vertical slice (indexed as 'i'), various forces and stresses come into play.

4.3. Normal and shear stresses on the base

Normal stress: denoted as 'Wi' and 'Pi'.
Shear stress: denoted as 'Ti' and 'Qi'.

4.4. Interslice normal and shear stresses

Normal stress between adjacent slices: represented as 'Xi' and 'Xi+1'.
Shear stress between adjacent slices: represented as 'Ei' and 'Ei+1'.

4.5. Soil shear strength

Soil shear strength is defined using the probabilistic Mohr-Coulomb failure criterion, which captures spatial variability globally.

4.6. Pore pressure

Pore pressures are taken into account, leading to corresponding reductions in normal effective stresses.

4.7. External forces

Seismic and traffic forces are transformed into equivalent shear stresses and applied to the bases of the slices.

4.8. Reinforcement stresses

Reinforcement stresses from the inclusions are integrated along the interfaces between beams and slices.

4.9. Factor of safety

A factor of safety 'F' is introduced to relate shear strengths to stresses.

4.10. Parameters for stress distribution

Two parameters, 'α' and 'λ' are introduced to distribute stresses in a way that satisfies the equilibrium of static moment and horizontal force.

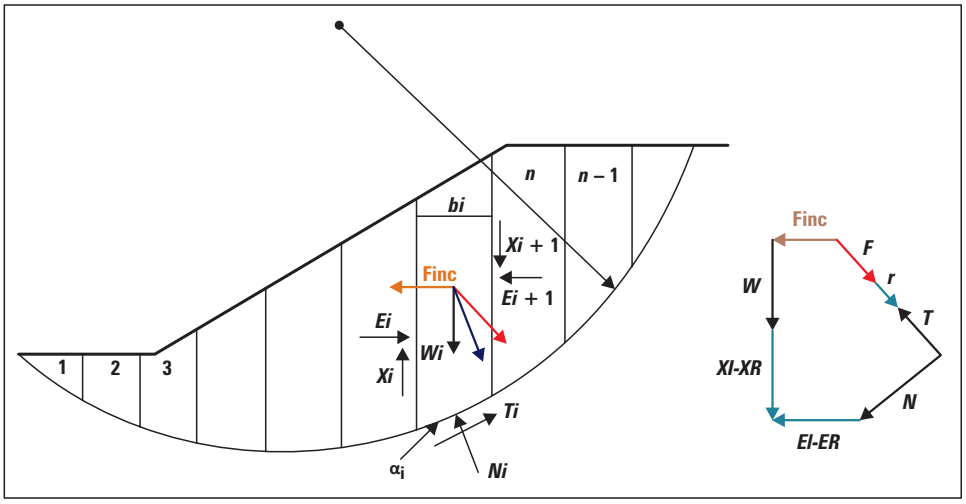

Source: Authors' own study

Fig. 3. a. Representation of an inclined slice being cut. **b.** Representation of the equilibrium state of a sliced section. **c.** Visualization of the force polygon with Xl, XR, EL, ER as interslice forces; W as the gravitational weight; N as the normal force; S as the shear resistance; Finc as the tensile force exerted by inclusions; Fs as the forces resulting from traffic loads; and r as the force attributable to fluid flow

4.11. Governing equilibrium equations

The equilibrium equations governing each vertical slice are as follows:

Force Equilibrium:
$\Sigma Ti = \Sigma Qi$ (Equation 4),

Moment Equilibrium:
$\Sigma Mi = \Sigma\ NiTi - \Sigma\ NiQi\lambda$ (Equation 5),

Stress Distribution Equations:
$\Sigma NiTi = ciAiF + (\sigma'i - ui)\tan\varphi'iAiF(1 - \alpha i) + \alpha i(\sigma'i, bi - ui)\ \tan\varphi'iAib$ (Equation 6).

4.12. Solver and analysis

To ensure static admissibility, an iterative nonlinear solver computes values for 'αi', 'λi', and 'F'. This iterative process enforces equilibrium conditions.

4.13. Complexity

Our extended model introduces several complexities and improvements over conventional methods.

4.14. Spatial variability

We incorporate probabilistic strength distributions to account for realistic variations in soil properties that influence stress redistribution.

4.15. Pore pressure effects

Transient pore pressures are considered to improve the modeling of effective stress conditions, that significantly affect shear strength mobilization.

4.16. Reinforcement inclusions

The mechanical representation of the inclusions allows us to quantify their influence on stress reduction along potential shear planes.

4.17. Dynamic loads

Equivalent seismic and traffic shear stresses are applied as slice base loads, accounting for the effects of transient dynamic stresses.

4.18. Full static admissibility

Both the force and the moment equilibrium with parameters 'α' and 'λ' are satisfied in accordance with the principles of limit analysis theory.

4.19. Non-uniform shear stress

The introduction of the 'α' term allows non-linear variations in shear stress along each slice, deviating from the assumption of a linear distribution.

4.20. Probabilistic analyses

The sensitivity and probabilistic analyses were performed to account for uncertainties in input parameters, extending beyond deterministic assessments.

$$S = 1/F(c'(w)\,\ell + N\tan\varphi'(w)) \tag{7}$$

The projection of forces on the vertical in the center of the slice.

$$(N + u_a \cdot \ell - \chi \cdot \ell \cdot s_e)\cos\alpha = W + (X_L - X_R) - S \cdot \sin\alpha + (F^s_{vert} + r\sin\theta) \tag{8}$$

With α: the angle of base of slice, θ: gradient of the piezometric level.
The replacement of the value of S from eq (7).

$$(N + u_a \cdot \ell - \chi \cdot \ell \cdot s_e)\cos\alpha = W + (x_l - x_r) - \sin\alpha/F(c'(w)\,\ell + \\ + N'\tan\varphi'(w)) + (F^s_{vert} + r\sin\theta) \tag{9}$$

$$(N\cos\alpha) + (u_a \cdot \ell - \chi \cdot \ell \cdot s_e)\cos\alpha = W + (x_L - x_R) - \\ - (c'(w)\,\ell\,/F\,)\sin\alpha - N\tan\varphi'(w)\sin\alpha\,/F) + (F^s_{vert} + r\sin\theta) \tag{10}$$

With c'(w), φ'(w) are residual characteristics due to material fatigue.

$$N(\cos\alpha + (\tan\varphi'(w)\sin\alpha)/F) = W + (x_L - x_R) - \\ - \ell\,(u_a - \chi \cdot s_e)\cos\alpha - c'(w)\,\sin\alpha\,/F\,) + (F^s_{vert} + r\sin\theta).$$

$$N = \frac{(W + (x_L - x_R) - 1(u_a - \chi \cdot s_e\cos\alpha - c'(w)\sin\alpha/F) + (Fs_{vert} + r\sin\theta)}{(\cos\alpha + (\tan\varphi'(w)\sin\alpha)/F} \tag{11}$$

For clarity and simplification, Bishop allowed to ignore the interslice forces (with a small difference between them) and set the center of gravity of the slice to his half height. The moments relative to the slippery mass rotation center are:

$$WR_x = S \cdot R - F^s_{vert}\,R_x - F^s_{horiz}(R\,(\cos\alpha) - h/2) - r\sin\theta R_x - \\ - r\,\cos\theta(R(\cos\,\alpha) - h/2) + F_{inc}(R(\cos\alpha) - h/2).$$

$$WR\,\sin\alpha = R \cdot \tau\ell - F^s_{vert}\,R\,\sin\alpha - F^s_{horiz}(R\,(\cos\alpha) - h/2) - \\ - ((r\sin\theta\,R\sin\alpha) + ((r\cos\theta - F_{inc})(R(\cos\alpha) - h/2))) \tag{12}$$

The introduction of Mohr-Coulomb criterion ($\tau = c' + \sigma \tan\varphi'$) in eq (12).

$$Wr\,\sin\alpha = R/F[(c'(w)\ell + N\,\tan\varphi'(w)\ell) - (\ell\tan\varphi'(w) \cdot (u_a - \chi \cdot s_e))] - \\ - [(F^s_{vert} + r\sin\theta)(R\,\sin\alpha)] - [(F^s_{horiz} + r\cos\theta - F_{inc}) \cdot (R\,(\cos\alpha) - h/2)] \tag{13}$$

$$F = \frac{R\left[\left(c'(w)\ell + N\cdot\tan\varphi'(w)\ell\right) - \left(\ell\tan\varphi'(w)\cdot(ua - \chi\cdot se)\right)\right]}{WR\,\sin\alpha + \left[(Fs_{vert} + r\sin\theta)(R\sin\alpha)\right] + \left[(Fs_{horiz} + r\cos\theta - G_{eo})\left(R\cdot(\cos\alpha) - \frac{h}{2}\right)\right]}$$

$$F = \frac{\left[c'(w)\ell + N\tan\varphi'(w)\right] - \left[\ell\tan\varphi'(w)\cdot(ua - \chi\cdot se)\right]}{WR\,\sin\alpha + \left[(Fs_{vert} + r\sin\theta)(R\sin\alpha)\right] + \left[(Fs_{horiz} + r\cos\theta - G_{eo})\left(R\cdot(\cos\alpha) - \frac{h}{2}\right)\right]} \tag{14}$$

By substituting the value of N taken from (11) in (14) and summing all slices:

$$F = \frac{\sum c'(w)\ell + \dfrac{\tan\varphi'(w)\left[W - \left(\ell\cos\alpha(ua - \chi\cdot se)\right)\right] + \left(c'(w)\sin\alpha/F\right) + Fs_{vert} + r\sin\theta}{\cos\alpha + \left(\tan\varphi'(w)\sin\alpha/F\right)} - \ell(ua - \chi\cdot se)}{\sum\left[W_i\sin\alpha_i + \left((Fs_{horiz} + r_i\cos\theta_i - G_{eo})\left(\cos\alpha_i - \dfrac{h_i}{2R}\right)\right) + (r_i\sin\theta_i + \sum Fs_{vert})(\sin\alpha_i)\right]} \tag{15}$$

The use of the term: $\dfrac{1}{m \propto} = \dfrac{\left(\sec\alpha\right)}{\left(1 + (\tan\varphi'(w) \cdot \tan\alpha)\right)}{F}$

$$F = \frac{\left(c'(w)\ell + N\tan\varphi'(w)\left(W - \ell\cos\alpha(ua - \chi\cdot se)\right)\right) + \left[\left(\left(\left(c'\frac{(w)\sin\alpha}{F}\right) + Fs_{vert} + r\sin\theta\right)\frac{1}{m_\alpha}\right) - \ell(ua - \chi\cdot se)\right]}{\sum W_i\sin\alpha_i + \left[\left(Fs_{horiz} + r_i\cos\theta_i - G_{eo}\right)\left(\cos\alpha_i - \frac{h_i}{2R}\right) + \left(r_i\sin\theta_i + \sum Fs_{vert}\right)\left(\sin\alpha_i\right)\right]} \quad (16)$$

$$F = \frac{\sum\left\{c'b + \tan\varphi'\left(W\left(1 - ru\right)\right)\right\}\frac{1}{m\alpha}}{\sum W\sin\alpha} \quad (17)$$

$$F = \frac{\sum\left\{c'b + \tan\varphi'\left(W\left(1 - ru\right)\right) + \left(xl - xr\right)\right\}\frac{1}{m\alpha}}{\sum W\sin\alpha} \quad (18)$$

$$\text{With } \varphi' = \varphi \cdot K_\varphi \text{ and } ru = \frac{u}{\text{total vertical stress}}$$

5. Results and discussions

The modified Bishop method relates the factor of safety F to the stabilizing shear strength parameters and driving stresses along the critical failure surface, accounting for spatially varying soil properties, pore pressures, seismic/traffic loads, and reinforcement inclusions:

$$F = (\Sigma T_i - \Sigma Q_i\lambda) / (\Sigma c_i A_i + \Sigma(\sigma'_i - u_i)\tan\varphi'_i A_i(1 - \alpha_i) + \\ + \Sigma\alpha_i(\sigma'_i, b_i - u_i)\tan\varphi'_i A_i b_i) \quad (19)$$

Where the terms in the numerator capture the resisting stresses and the denominator represents the driving stresses modified by the input probabilistic distributions. Finite element discretization of the potential failure mass allows iterative solution of equations (6–7) through Newton-Raphson stabilization to satisfy static admissibility.

Probabilistic Monte Carlo simulations are performed in order to stochastically evaluate the stability performance over thousands of randomized input parameter realizations. This results in probability distributions and statistical moments of F, which incorporate the assessment of joint input uncertainties.

Sensitivity analyses assess the most significant geotechnical parameter influences through variance-based dimensionality reduction. Numerical location of critical slip surfaces is achieved by minimizing F through optimization.

Results demonstrate improved characterization of the stress conditions driving slope instability compared to traditional limit equilibrium methods. Probabilistic outputs inform robust risk quantification and design under conditions of uncertainty.

The modified Bishop equation accounts for spatially varying soil properties through the use of probabilistic distributions in the shear strength terms:

The shear strength parameters c' and φ' are assigned random values from probabilistic distributions rather than single mean values.

These distributions capture the natural variability in properties obtained from site investigation data (e.g. normal, lognormal distributions fit to measurement data).

When calculating the shear strength terms for each slice i in the equation:

$$\Sigma\, c_i A_i + \Sigma(\sigma'_I - u_i) \tan\varphi'_I A_i (1 - \alpha_i) + \Sigma\alpha_i (\sigma'_i, b_i - u_i) \tan\varphi'_I A_i b_i$$

The cohesion ci and friction angle φ'i are randomly sampled for each slice from the respective c' and φ' distributions. This assigns spatially the varying shear strength values along the failure surface based on the statistical characterization of the property heterogeneity.

Monte Carlo simulations propagate this variability in strengths into probabilistic estimates of the factor of safety. The spatially random strengths better represent real conditions than uniform mean values. By incorporating property variations into a probabilistic framework, the model accounts for their natural distributions and the resulting impact on slope stability.

Some common probabilistic distributions that can be used to characterize the spatial variability of shear strength parameters include:

Normal distribution: Often used for cohesion (c'), where the property values cluster around a mean in a Gaussian-like fashion.

Log-normal distribution: Suitable for friction angle (φ') and other positive-valued properties with log-transformed data following a normal distribution.

Uniform distribution: Can represent complete uncertainty over a range when little data is available to infer a distinct distribution shape.

Beta distribution: Flexible distribution that can take on different shapes to fit skewed or bimodal data patterns not captured by normal/lognormal.

Gamma distribution: Used for non-negative properties where variability increases with magnitude, such as c' influenced by soil composition percentages.

Weibull distribution: Applies when failures are characterized by the weakest-link phenomena, such as shear strength, which is governed by fault planes/defects.

Expert elicitation: When data is scarce, expert opinions on ranges/probability densities can inform distributions.

The appropriate distribution is selected based on techniques, such as probability plotting, maximum likelihood or Bayesian model selection applied to available shear strength measurements.

6. Conclusions

This study has presented an advanced mathematical approach within the field of Landscape Mechanics that aims to revolutionize our understanding of slope stability analysis. The extended limit equilibrium framework, based on the modified Bishop approach, stands as the pinnacle of mathematical rigor in the field. Its profound impact lies in its ability to address the complex realities of slope stability under diverse conditions. At its core, this approach goes beyond traditional methodologies by considering intricate facets of instability trigger mechanisms. It overcomes the constraints of average

properties by embracing spatial variability, thereby faithfully representing the inherent heterogeneity found in real-world landscapes. By careful consideration of the transient pore pressure influences by rigorous hydrological modeling, it frees the analysis from the constraints of assumptions typical for stable states. It is also not limited by the empirical strength increases thanks to mechanically modeled reinforcement structures. It deftly balances both the force and the moment equilibria with unparalleled precision through automated numerical solutions. This contrasts with the traditional reliance on approximate analytical methods, ushering in a new era of accuracy. The model's ability to handle non-linear shear stress distributions, as opposed to the limiting linear assumptions, marks a significant departure from the norm. Additionally, it introduces a probabilistic paradigm that accounts for the inherent uncertainties in geotechnical properties and loads. This shift from deterministic analyses to probabilistic characterization is transformative. Through Monte Carlo simulations, the model seamlessly propagates these uncertainties, computing robust stability risk estimates. This is a significant improvement over traditional methods that have often overlooked these critical factors. The model gives engineers and researchers the tools to systematically identify key influences on stability through sensitivity and uncertainty analyses. In practical terms, this mathematical formulation finds broad application across a spectrum of natural and engineered slope scenarios. From the protection of natural slopes against rainfall-induced landslides to the strengthening of anthropic structures, such as transportation embankments, its utility knows no bounds. The modified mathematical approach, nestled within a probabilistic mechanics-based framework, represents a quantum leap in limit equilibrium slope stability analysis. It elegantly bridges the chasm between theory and reality, ushering in a new era of geohazard evaluation and mitigation design. Validated through rigorous field measurements, this model enhances our ability to understand and predict instability, promising a brighter future of safer, more resilient landscapes. The horizon of possibilities invites further integration with hydro-mechanical and seismic wave propagation models for fully dynamic slope response simulations, underscoring its limitless potential in advancing the field of Landscape Mechanics.

Acknowledgements

This research was conducted under the guidance of the Laboratory of Applied Research in Engineering Geology, Geotechnics, Water Sciences, and Environment at Setif 1 University, Algeria. The authors wish to extend their sincere appreciation to the editor and the reviewers for their valuable input, which greatly improved the overall quality of this manuscript.

References

Anis Z., Wissem G., Riheb H., Biswajeet P., Essghaier G.M. 2019. Effects of clay properties in the landslides genesis in flysch massif: Case study of Aïn Draham, North Western Tunisia. Journal of African Earth Sciences, 151, 146–152.

Bishop A.W. 1955. The use of the slip circle in the stability analysis of slopes. Geotechnique, 5(1), 7–17.

Boubazine L., Boumazbeur A., Hadji R., Fares K. 2022. Slope failure characterization: A joint multi-geophysical and geotechnical analysis. Case study of Babor Mountains range, NE Algeria. Mining of Mineral Deposits, 16(4).

Brahmi S., Baali F., Hadji R., Brahmi S., Hamad A., Rahal O., ... Hamed Y. 2021. Assessment of groundwater and soil pollution by leachate using electrical resistivity and induced polarization imaging survey. Case of Tebessa municipal landfill, NE Algeria. Arabian Journal of Geosciences, 14, 1–13.

Charles J.A., Soares M.M. 1984. The stability of slopes in soils with nonlinear failure envelopes. Canadian Geotechnical Journal, 21(3), 397–406.

Dahoua L., Usychenko O., Savenko V.Y., Hadji R. 2018. Mathematical approach for estimating the stability of geotextile-reinforced embankments during an earthquake. Mining Science, 25, 207–217.

Dahoua L., Yakovitch S.V., Hadji R.H. 2017. GIS-based technic for roadside-slope stability assessment: An bivariate approach for A1 East-West highway, North Algeria. Mining Science, 24.

Fredj M., Hafsaoui A., Riheb H., Boukarm R., Saadoun A. 2020. Back-analysis study on slope instability in an open pit mine (Algeria). Natsional'nyi Hirnychyi Universytet. Naukovyi Visnyk, (2), 24–29.

Hadji R., Boumazbeur A., Limani Y., Baghem M., Chouabi A. 2013. Geologic, topographic and climatic controls in landslide hazard assessment using GIS modeling: A case study of Souk Ahras region, NE Algeria. Quaternary International, 302, 224–237.

Hadji R., Chouabi A., Gadri L., Raïs K., Hamed Y., Boumazbeur A. 2016. Application of linear indexing model and GIS techniques for the slope movement susceptibility modeling in Bousselam upstream basin, Northeast Algeria. Arabian Journal of Geosciences, 9, 192.

Hadji R., Rais K., Gadri L., Chouabi A., Hamed Y. 2017. Slope failure characteristics and slope movement susceptibility assessment using GIS in a medium scale: A case study from Ouled Driss and Machroha municipalities, Northeast Algeria. Arabian Journal for Science and Engineering, 42(1), 281–300.

Kallel A., Ksibi M., Dhia H.B., Khélifi N. (eds.). 2018. Recent advances in environmental science from the Euro-Mediterranean and surrounding regions. Proceedings of Euro-Mediterranean Conference for Environmental Integration (EMCEI-1), Tunisia 2017. Springer International Publishing.

Karim Z., Hadji R., Hamed Y. 2019. GIS-based approaches for the landslide susceptibility prediction in Setif Region (NE Algeria). Geotechnical and Geological Engineering, 37(1), 359–374.

Kerbati N.R., Gadri L., Hadji R., Hamad A., Boukelloul M.L. 2020. Graphical and numerical methods for stability analysis in surrounding rock of underground excavations. Example of Boukhadra Iron Mine NE Algeria. Geotechnical and Geological Engineering, 38, 2725–2733.

Mahleb A., Hadji R., Zahri F., Boudjellal R., Chibani A., Hamed Y. 2022. Water-Borne Erosion Estimation Using the Revised Universal Soil Loss Equation (RUSLE) Model Over a Semiarid Watershed: Case Study of Meskiana Catchment, Algerian-Tunisian Border. Geotechnical and Geological Engineering, 40(8), 4217–4230.

Manchar N., Benabbas C., Hadji R., Bouaicha F., Grecu F. 2018. Landslide Susceptibility Assessment in Constantine Region (NE Algeria) by Means of Statistical Models. Studia Geotechnica et Mechanica, 40(3), 208–219.

Mestat P. 1998. Du bon usage de l'élasticité dans les calculs de géotechnique. La pratique des calculs tridimensionnels en géotechnique. Presses de l'école nationale des Ponts et chaussées. Eds. J.P. Magnan, A. Guilloux, P. Mestat, 241, 256.

Morgenstern N.U., Price V.E. 1965. The analysis of the stability of general slip surfaces. Geotechnique, 15(1), 79–93.

Ncibi K., Hadji R., Hajji S., Besser H., Hajlaoui H., Hamad A., ... Hamed Y. 2021. Spatial variation of groundwater vulnerability to nitrate pollution under excessive fertilization using index overlay method in central Tunisia (Sidi Bouzid basin). Irrigation and Drainage, 70(5), 1209–1226.

Saadoun A., Yilmaz I., Hafsaoui A., Hadji R., Fredj M., Boukarm R., Nakache R. 2020. Slope stability study in quarries by different approaches: Case Chouf Amar Quarry, Algeria. IOP Conference Series: Materials Science and Engineering, 960, 4, 042026. IOP Publishing.

Terzaghi K., Peck R.B. 1967. Soil mechanics in engineering practice. No. 624.151 T47 1967.

Zahri F., Boukelloul M.L., Hadji R., Talhi K. 2016. Slope stability analysis in open pit mines of Jebel Gustar career, NE Algeria. A multi-steps approach. Mining Science, 23.

Zeqiri R.R., Riheb H., Karim Z., Younes G., Rania B., Aniss M. 2019. Analysis of safety factor of security plates in the mine 'Trepça' Stantërg. Mining Science, 26, 21.

PhD Larbi Khaber
University of Farhat Abbas
Department of Earth Sciences
Institute of Architecture and Earth Sciences, Algeria
e-mail: khaber2013@gmail.com

PhD Karim Zighmi
University of Farhat Abbas, Algeria
Laboratory of Applied Research in Engineering Geology,
Geotechnics, Water Sciences, and Environment
Department of Earth Sciences
Institute of Architecture and Earth Sciences
e-mail: zighmi.karim19@gmail.com

PhD Riheb Hadji
University of Farhat Abbas, Algeria
Laboratory of Applied Research in Engineering Geology, Geotechnics,
Water Sciences, and Environment
Department of Earth Sciences
Institute of Architecture and Earth Sciences
e-mail: hadjirihab@gmail.com